

Semicoherent searches for continuous gravitational waves: improving robustness versus transient disturbances and increasing sensitivity to transient signals

David Keitel*

Albert-Einstein-Institut, Callinstraße 38, 30167 Hannover, Germany

(Dated: 08 September 2015)

(LIGO document number: LIGO-P1500159)

The vulnerability of standard detection methods for long-duration quasi-monochromatic gravitational waves from non-axisymmetric rotating neutron stars (‘continuous waves’, *CWs*) to single-detector instrumental artifacts was addressed in past work [Keitel, Prix, Papa, Leaci and Siddiqi, Phys. Rev. D **89**, 064023 (2014)] by a Bayesian approach. An explicit model of persistent single-detector disturbances led to a generalized detection statistic with improved robustness against such artifacts. Since many strong outliers in semicoherent searches of LIGO data are caused by transient disturbances that last only a few hours, we extend this approach to cover transient disturbances, and demonstrate increased robustness in realistic simulated data. Besides long-duration *CWs*, neutron stars could also emit transient signals which, for a limited time, also follow the *CW* signal model (*tCWs*). As a pragmatic alternative to specialized transient searches, we demonstrate how to make standard semicoherent *CW* searches more sensitive to transient signals. Focusing on the time-scale of a single segment in the semicoherent search, Bayesian model selection yields a generalized detection statistic that does not add significant computational cost. On simulated data, we find it to increase sensitivity towards *tCWs*, without sacrificing sensitivity to classical *CW* signals, and still being robust to transient or persistent single-detector instrumental artifacts.

PACS numbers: 04.30.Tv, 04.80.Nn, 95.55.Ym, 97.60.Jd

I. INTRODUCTION

Among the main search targets of terrestrial interferometric detectors [1–5] are continuous gravitational waves (*CWs*): periodic, narrow-band signals with a slow frequency evolution, emitted by rotating neutron stars with non-axisymmetric deformations. [6, 7] Searches for *CWs* from unknown sources over wide parameter spaces are usually performed with *semicoherent* methods. [8–11] For these, the data is split into several shorter *segments*, each segment analyzed coherently, and the resulting per-segment detection statistics combined incoherently, e.g. by a sum. At fixed computational cost, semicoherent methods are generally more sensitive than fully-coherent searches. [8, 9, 12]

Even though gravitational-wave detectors are highly precise instruments, they still produce complicated data sets with many noise components. These are not all fully modeled by existing data analysis procedures, and thus result in *outliers* of the detection statistics. To distinguish these from real signals, labor-intensive manual follow-up is often necessary. Outliers in *CW* searches are often caused by so-called *lines*, narrow-band disturbances that are typically present for a sizable fraction of the observation time. Lines can have diverse instrumental or environmental origins, such as harmonics of the electrical power grid frequency, of the detector’s suspension system, or from digital components. [13–18]

However, in a semicoherent search for *CWs* from the galactic center with LIGO S5 data [19–21], based on the

global-correlations (GCT) search method [11, 22], it was noticed that many strong outliers can actually be traced back to disturbances in the data happening only within a single segment. Similar transient disturbances have also been found in LIGO S6 data. [23] (Note that this class of ‘transient’ disturbances are of much longer duration than the typical ‘glitches’ which influence the performance of searches for compact-binary coalescences and ‘burst’-type signals. [15, 24–26])

Hence, in the galactic-center search a *permanence veto* was introduced. [19–21] It removes any candidates for which a single segment contributes excessively to the semicoherent detection statistic. Based on the single-segment, *multi-detector coherent* statistics, the permanence veto was proven to be very effective, and also safe regarding classical *CW* signals, which are persistent over timescales comparable to the full length of the data set. [19–21] However, in a semicoherent *CW* search over several months of data, such a veto also suppresses medium-duration signals, active for only a few hours or days: these would produce just the same data signature in terms of single-segment, *multi-detector* statistics. Such ‘transient-*CW*’ signals (*tCWs*), following the standard *CW* signal model but for a limited duration, are also considered as viable candidates for detection [27, 28], with several possible emission mechanisms from perturbed neutron stars [29–34].

Therefore, in this paper we investigate an alternative approach to the permanence veto, constructing a detection statistic that is robust against *single-detector* transient artifacts, while at the same time being more sensitive than standard statistics to transient signals that are coherent across multiple detectors.

* David.Keitel@ligo.org

In the literature, two methods for detecting tWC signals have been proposed: On the one hand, a coherent \mathcal{F} -statistic-based CW search with transient duration, start-time and shape as additional phase-evolution parameters. [27, 28] This is a nearly optimal approach, but computationally expensive. On the other hand, unmodeled ‘excess power’ detection methods originally used to search for GW bursts of at most a few seconds have recently been extended to cover longer durations. [35] These could also have potential for detecting tCWs, although there is no direct comparison of sensitivity yet. Neither of these approaches has yet been used for an analysis of actual interferometer data.

Our approach is a pragmatic extension of the *line-robust statistics* of Ref. [36] (hereafter Paper I), which in turn are based on the standard matched-filter \mathcal{F} -statistic [37, 38]. The \mathcal{F} -statistic is close to optimal as a detection statistic for persistent CWs in Gaussian noise [39], which in current detectors is a good model for the noise distribution over most of the observation time and frequency range. (See, e.g., Refs. [17, 21, 40]). In fact, the \mathcal{F} -statistic corresponds to a binary hypothesis test between a CW signal hypothesis and a Gaussian-noise hypothesis. [39]

In the line-robust statistics from Paper I, the noise model is extended to include persistent single-detector lines, without any detailed physical modeling of the lines’ origin: the idea is to simply model a line as identical to a CW signal, but confined to a single detector. We summarize these developments in Sec. II.

In Sec. III of this paper, we further extend the noise model of that approach to also include transient disturbances – or, more specifically: single-segment, single-detector disturbances. With this approach, we can make our detection methods more *robust* towards both persistent and transient single-detector disturbances. It can reproduce the robustness of the permanence veto when considering persistent CW signals only, while not being as strict in suppressing transient tCW signals. In a second step, described in Sec. IV, we aim to recover full sensitivity towards transient signals, and in fact to *improve* it compared to standard semicoherent methods. We achieve this by also including an explicit signal model for transient CW-like signals on a time-scale corresponding to a single segment in a semicoherent search. We then test these extended detection statistics in Sec. V, using simulated data with a realistic distribution of gaps in observation times, and conclude in Sec. VI.

II. SUMMARY OF EXISTING SEMICOHERENT DETECTION STATISTICS

In this section, we briefly summarize how the established \mathcal{F} -statistic [37, 38] can be re-derived from a Bayesian hypothesis testing approach [39], and how this approach was extended to produce line-robust detection statistics in Paper I.

This section also serves as an introduction to the notation used in this paper. By $x^X(t)$ we denote a time series of GW strain measured in a detector X . Following the multi-detector notation of [38, 41], boldface indicates a multi-detector vector, i.e., we write $\mathbf{x}(t)$ for the multi-detector data vector with components $x^X(t)$.

For Bayesian hypothesis testing [42], we use the following notations: $P(\mathcal{H}|x, \mathcal{I})$ is the probability of a hypothesis \mathcal{H} given data x and prior information \mathcal{I} . Posterior odds ratios between two hypotheses $\mathcal{H}_A, \mathcal{H}_B$ are written with an upper-case symbol $O_{A/B}(x, \mathcal{I})$; if \mathcal{H}_B is the logical sum of two hypotheses, $\mathcal{H}_B = (\mathcal{H}_C \text{ or } \mathcal{H}_D)$, we write $O_{A/B}(x, \mathcal{I}) = O_{A/CD}(x, \mathcal{I})$. The corresponding prior odds take a lower-case symbol, $o_{A/B}(\mathcal{I})$, and the likelihood ratio or *Bayes factor* is $B_{A/B}(x, \mathcal{I})$, so that $O_{A/B}(x, \mathcal{I}) = o_{A/B}(\mathcal{I}) B_{A/B}(x, \mathcal{I})$.

Also, in this paper we indicate semicoherent quantities from a search with a number N_{seg} of segments with a hat, such as $\widehat{\mathcal{F}}$. Coherent single-segment quantities are indicated by a tilde above the symbol and an upper index $\ell = 1 \dots N_{\text{seg}}$ enumerating the segments, such as $\widetilde{\mathcal{F}}^\ell$.

A. The $\widehat{\mathcal{F}}$ -statistic: signals in Gaussian noise

We start with a *Gaussian-noise hypothesis*, $\widehat{\mathcal{H}}_G : \mathbf{x}(t) = \mathbf{n}(t)$, with the samples of $\mathbf{n}(t)$ drawn from a Gaussian distribution. Its posterior probability, given priors $P(\widehat{\mathcal{H}}_G|\mathcal{I})$ and $P(\mathbf{x}|\mathcal{I})$, is

$$P(\widehat{\mathcal{H}}_G|\mathbf{x}, \mathcal{I}) = \frac{P(\widehat{\mathcal{H}}_G|\mathcal{I})}{P(\mathbf{x}|\mathcal{I})} \kappa e^{-\frac{1}{2}(\mathbf{x}|\mathbf{x})}, \quad (1)$$

with a normalization constant κ and a scalar product between time series defined as

$$(\mathbf{x}|\mathbf{y}) \equiv \sum_{X=1}^{N_{\text{det}}} \frac{1}{S^X} \int_0^T x^X(t) y^X(t) dt. \quad (2)$$

Here, S^X is the single-sided power-spectral densities, assumed as uncorrelated between different detectors and constant over the (narrow) frequency band of interest.

The *CW signal hypothesis*

$$\widehat{\mathcal{H}}_S : \mathbf{x}(t) = \mathbf{n}(t) + \mathbf{h}(t; \mathcal{A}, \lambda) \quad (3)$$

contains a waveform with a set \mathcal{A} of 4 *amplitude parameters* and a set λ of *phase-evolution parameters* (including frequency, spin-down and sky position). In a semicoherent search, different \mathcal{A}^ℓ are allowed in each segment; but we simplify our notation by re-defining $\mathcal{A} = \{\mathcal{A}^\ell\}$.

After marginalizing over \mathcal{A} and the associated prior (cf. [27, 36, 39, 43]), the posterior probability is

$$P(\widehat{\mathcal{H}}_S|\mathbf{x}, \mathcal{I}) = \widehat{o}_{S/G}(\mathcal{I}) P(\widehat{\mathcal{H}}_G|\mathbf{x}, \mathcal{I}) e^{\widehat{\mathcal{F}}(\mathbf{x}) - N_{\text{seg}} \mathcal{F}_*^{(0)}}. \quad (4)$$

Here, $\widehat{o}_{S/G}(\mathcal{I}) \equiv P(\mathcal{H}_S|\mathcal{I})/P(\mathcal{H}_G|\mathcal{I})$ are the prior odds between a signal and Gaussian noise; $\mathcal{F}_*^{(0)} \in (-\infty, \infty)$

is a free parameter (the result of an arbitrary \mathcal{A} -prior cutoff); and the semicoherent multi-detector $\widehat{\mathcal{F}}$ -statistic is, for a single parameter-space point λ , given by the sum over single-segment coherent $\widetilde{\mathcal{F}}^\ell$ -statistics:

$$\widehat{\mathcal{F}}(\mathbf{x}; \lambda) \equiv \sum_{\ell=1}^{N_{\text{seg}}} \widetilde{\mathcal{F}}^\ell(\mathbf{x}^\ell; \lambda). \quad (5)$$

In practice, often an *interpolating StackSlide* algorithm is used, where $\widehat{\mathcal{F}}(\mathbf{x}; \lambda)$ for each λ is computed from a set of $\widetilde{\mathcal{F}}^\ell(\mathbf{x}^\ell; \lambda^\ell)$ with the λ^ℓ picked from a coarser grid in parameter space than the λ . [8, 9, 11, 12]. In Eq. (4), as well as for the rest of the paper, we do not explicitly show the λ -dependence of our detection statistics.

These posterior probabilities can be used to compute odds ratios between the different hypotheses. First, we see from Eqs. (1) and (4) that

$$\widehat{O}_{S/G}(\mathbf{x}, \mathcal{I}) \equiv \frac{P(\widehat{\mathcal{H}}_S | \mathbf{x}, \mathcal{I})}{P(\widehat{\mathcal{H}}_G | \mathbf{x}, \mathcal{I})} \propto \widehat{B}_{S/G}(\mathbf{x}, \mathcal{I}) \propto e^{\widehat{\mathcal{F}}(\mathbf{x})}, \quad (6)$$

i.e., this Bayesian approach reproduces the $\widehat{\mathcal{F}}$ -statistic as the optimal detection statistic for CW signals in pure Gaussian noise and under the assumed priors. The free parameter $\mathcal{F}_*^{(0)}$ is irrelevant in this case.

B. Permanence veto

The permanence veto, as introduced in Refs. [19–21], works by the following algorithm: From a fixed Gaussian false-alarm level or some real-data noise studies, a threshold $\overline{\mathcal{F}}_{\text{thr}}$ is set on the average semicoherent statistic $\overline{\mathcal{F}} \equiv \widehat{\mathcal{F}}/N_{\text{seg}}$. Then, for each candidate the highest single-segment contribution is removed, defining

$$\overline{\mathcal{F}}_{\text{pv}}(\mathbf{x}; \lambda) \equiv \frac{1}{N_{\text{seg}} - 1} \sum_{\ell \neq m} \widetilde{\mathcal{F}}^\ell(\mathbf{x}^\ell; \lambda^\ell). \quad (7)$$

where m is the segment with the highest multi-detector $\widetilde{\mathcal{F}}^m \equiv \max_{\ell} \widetilde{\mathcal{F}}^\ell$.

In the original implementation of Refs. [19–21], the $\overline{\mathcal{F}}_{\text{pv}}$ value of each candidate is compared with the threshold $\overline{\mathcal{F}}_{\text{thr}}$ to determine whether to veto the candidate. In our tests in Sec. V, we slightly modify this algorithm to treat the permanence veto on a more equal footing with the other detection statistics: We define $\overline{\mathcal{F}}_{\text{pv}}$ exactly as in Eq. (7), but we set a detection threshold by computing the maximum of $\overline{\mathcal{F}}_{\text{pv}}$ over a pure-noise data set.

C. Line-robust statistics

The noise model is more general when including a simple non-coincident *‘line’ hypothesis* $\widehat{\mathcal{H}}_L^X : x^X(t) = n^X(t) + h^X(t; \mathcal{A}^X)$, which just assumes a

CW-like disturbance in an arbitrary single detector X . A similar derivation leads to

$$P(\widehat{\mathcal{H}}_L | \mathbf{x}, \mathcal{I}) = P(\widehat{\mathcal{H}}_G | \mathbf{x}, \mathcal{I}) \sum_{X=1}^{N_{\text{det}}} \widehat{o}_{L/G}^X e^{\widehat{\mathcal{F}}^X(x^X) - N_{\text{seg}} \mathcal{F}_*^{(0)}}, \quad (8)$$

with the per-detector line-prior odds and their sum,

$$\widehat{o}_{L/G}^X(\mathcal{I}) \equiv P(\widehat{\mathcal{H}}_L^X | \mathcal{I}) / P(\widehat{\mathcal{H}}_G^X | \mathcal{I}), \quad (9a)$$

$$\widehat{o}_{L/G}(\mathcal{I}) \equiv \sum_X \widehat{o}_{L/G}^X(\mathcal{I}). \quad (9b)$$

We suppress the \mathcal{I} -dependence of any odds ratios or Bayes factors in Eq. (8) and from now on.

Furthermore, we can combine the (mutually exclusive) hypotheses $\widehat{\mathcal{H}}_G$ and $\widehat{\mathcal{H}}_L$ into an extended noise hypothesis $\widehat{\mathcal{H}}_{GL} \equiv (\widehat{\mathcal{H}}_G \text{ or } \widehat{\mathcal{H}}_L)$, with posterior probability

$$P(\widehat{\mathcal{H}}_{GL} | \mathbf{x}, \mathcal{I}) = P(\widehat{\mathcal{H}}_G | \mathbf{x}, \mathcal{I}) + P(\widehat{\mathcal{H}}_L | \mathbf{x}, \mathcal{I}) \quad (10)$$

$$= P(\widehat{\mathcal{H}}_G | \mathbf{x}, \mathcal{I}) \left(1 + \sum_{X=1}^{N_{\text{det}}} \widehat{o}_{L/G}^X e^{\widehat{\mathcal{F}}^X(x^X) - N_{\text{seg}} \mathcal{F}_*^{(0)}} \right).$$

Finally, using Eqs. (4) and (10), we obtain generalized signal-versus-noise odds

$$\widehat{O}_{S/GL}(\mathbf{x}) = \frac{\widehat{O}_{S/G} e^{\widehat{\mathcal{F}}(\mathbf{x})}}{e^{N_{\text{seg}} \mathcal{F}_*^{(0)}} + \sum_X \widehat{o}_{L/G}^X e^{\widehat{\mathcal{F}}^X(x^X)}} \quad (11)$$

and, with the conditional probabilities for lines in the absence of a signal,

$$\widehat{p}_L \equiv P(\widehat{\mathcal{H}}_L | \widehat{\mathcal{H}}_{GL}, \mathcal{I}) = \frac{\widehat{o}_{L/G}}{1 + \widehat{o}_{L/G}}, \quad (12a)$$

$$\widehat{p}_L^X \equiv P(\widehat{\mathcal{H}}_L^X | \widehat{\mathcal{H}}_{GL}, \mathcal{I}) = \frac{\widehat{o}_{L/G}^X}{1 + \widehat{o}_{L/G}^X}, \quad (12b)$$

the corresponding Bayes factor, or *line-robust statistic*, is

$$\widehat{B}_{S/GL}(\mathbf{x}) = \frac{e^{\widehat{\mathcal{F}}(\mathbf{x})}}{(1 - \widehat{p}_L) e^{N_{\text{seg}} \mathcal{F}_*^{(0)}} + \sum_X \widehat{p}_L^X e^{\widehat{\mathcal{F}}^X(x^X)}}. \quad (13)$$

Contrary to $\widehat{O}_{S/G}$ or $\widehat{B}_{S/G}$, now the parameter $\mathcal{F}_*^{(0)}$ (from the amplitude-prior cutoff) will affect the properties of the resulting statistic, determining a transition scale between increased strictness to either Gaussian noise or lines. Methods for tuning this parameter, and the $\widehat{o}_{L/G}^X$, are discussed in section VI.B of Paper I.

The limit of $\mathcal{F}_*^{(0)} \rightarrow -\infty$ corresponds to a binary test of \mathcal{H}_S against \mathcal{H}_L , excluding Gaussian noise. We refer to this Bayes factor $B_{S/L}$ as the *pure line-veto statistic*.

III. LINE-ROBUST STATISTIC FOR SINGLE-SEGMENT DISTURBANCES

Now we turn to the issue of non-coincident transient line-like disturbances. To address it in the same Bayesian framework as above, consider a new ‘*transient-line*’ hypothesis $\tilde{\mathcal{H}}_{\text{tL}}^{X\ell}$ for a quasi-harmonic disturbance in a single segment ℓ and single detector X :

$$\tilde{\mathcal{H}}_{\text{tL}}^{X\ell} : x^{X\ell}(t) = n^{X\ell}(t) + h^{X\ell}(t; \mathcal{A}^{X\ell}). \quad (14)$$

This is just the full CW hypothesis from Eq. (3) restricted to a subset $x^{X\ell}(t)$ of the data. Thus, in analogy with Eqs. (4) and (8) and dropping the time-series arguments again, the posterior probability for $\tilde{\mathcal{H}}_{\text{tL}}^{X\ell}$ is

$$P\left(\tilde{\mathcal{H}}_{\text{tL}}^{X\ell} \middle| x^{X\ell}, \mathcal{I}\right) = P\left(\tilde{\mathcal{H}}_{\text{G}}^{X\ell} \middle| x^{X\ell}, \mathcal{I}\right) \tilde{\omega}_{\text{tL/G}}^{X\ell} e^{\tilde{\mathcal{F}}^{X\ell}(x^{X\ell}) - \mathcal{F}_*^{(0)}}. \quad (15)$$

In principle, we could now build up a wide range of composite hypotheses about the whole data-set \mathbf{x} – spanning $N_{\text{seg}} \times N_{\text{det}}$ subsets $x^{X\ell}(t)$ – by combining instances of $\tilde{\mathcal{H}}_{\text{tL}}^{X\ell}$ and of the single-segment Gaussian-noise hypothesis $\tilde{\mathcal{H}}_{\text{G}}^{X\ell}$, and by setting appropriate constraints on the amplitude parameters $\{\mathcal{A}^{X\ell}\}$.

For example, the hypothesis $\hat{\mathcal{H}}_{\text{L}}$ for persistent single-detector lines corresponds to $\prod_{\ell} \tilde{\mathcal{H}}_{\text{tL}}^{X\ell}$ with the same $\mathcal{A}^{Y\ell}$ for all ℓ , but only for a specific detector $X = Y$; combined with $\prod_{\ell} \tilde{\mathcal{H}}_{\text{G}}^{X\ell}$ for all other detectors $X \neq Y$.

However, now we will concentrate on one specific *new* full-dataset hypothesis $\hat{\mathcal{H}}_{\text{tL}}$: for the case of a transient, single-detector disturbance in only one ℓ and one X , with no prior constraint on the values of these indices. For example, if we have data in 2 segments for 2 detectors, the full hypothesis is

$$\begin{aligned} \hat{\mathcal{H}}_{\text{tL}} : & \left(\tilde{\mathcal{H}}_{\text{tL}}^{11} \text{ and } \tilde{\mathcal{H}}_{\text{G}}^{12} \text{ and } \tilde{\mathcal{H}}_{\text{G}}^{21} \text{ and } \tilde{\mathcal{H}}_{\text{G}}^{22} \right) \\ & \text{or } \left(\tilde{\mathcal{H}}_{\text{G}}^{11} \text{ and } \tilde{\mathcal{H}}_{\text{tL}}^{12} \text{ and } \tilde{\mathcal{H}}_{\text{G}}^{21} \text{ and } \tilde{\mathcal{H}}_{\text{G}}^{22} \right) \\ & \text{or } \left(\tilde{\mathcal{H}}_{\text{G}}^{11} \text{ and } \tilde{\mathcal{H}}_{\text{G}}^{12} \text{ and } \tilde{\mathcal{H}}_{\text{tL}}^{21} \text{ and } \tilde{\mathcal{H}}_{\text{G}}^{22} \right) \\ & \text{or } \left(\tilde{\mathcal{H}}_{\text{G}}^{11} \text{ and } \tilde{\mathcal{H}}_{\text{G}}^{12} \text{ and } \tilde{\mathcal{H}}_{\text{G}}^{21} \text{ and } \tilde{\mathcal{H}}_{\text{tL}}^{22} \right). \end{aligned} \quad (16)$$

The full semicoherent posterior probability for this hypothesis is then

$$\begin{aligned} P\left(\hat{\mathcal{H}}_{\text{tL}} \middle| \mathbf{x}, \mathcal{I}\right) &= \sum_{X\ell} P\left(\tilde{\mathcal{H}}_{\text{tL}}^{X\ell} \middle| x^{X\ell}, \mathcal{I}\right) \prod_{\substack{Y \neq X \\ \text{or } \ell' \neq \ell}} P\left(\tilde{\mathcal{H}}_{\text{G}}^{Y\ell'} \middle| x^{Y\ell'}, \mathcal{I}\right) \\ &= P\left(\hat{\mathcal{H}}_{\text{G}} \middle| \mathbf{x}, \mathcal{I}\right) \sum_{X\ell} \tilde{\omega}_{\text{tL/G}}^{X\ell} e^{\tilde{\mathcal{F}}^{X\ell} - \mathcal{F}_*^{(0)}}, \end{aligned} \quad (17)$$

introducing the shorthand notation $\sum_{X\ell} \equiv \sum_{\ell=1}^{N_{\text{seg}}} \sum_{X=1}^{N_{\text{det}}}$.

We can then produce a combined noise hypothesis $\hat{\mathcal{H}}_{\text{GLtL}}$ that allows for either pure Gaussian noise, a persistent line or a single-segment transient line:

$$\hat{\mathcal{H}}_{\text{GLtL}} : \left(\hat{\mathcal{H}}_{\text{G}} \text{ or } \hat{\mathcal{H}}_{\text{L}} \text{ or } \hat{\mathcal{H}}_{\text{tL}} \right). \quad (18)$$

As seen before in Paper I, $\mathcal{H}_{\text{L}}^X(\mathcal{A}^X)$ has the same likelihood as \mathcal{H}_{G}^X in the special case of vanishing amplitude parameters, $\mathcal{A}^X = 0$. But when we obtain the full line hypothesis \mathcal{H}_{L}^X by marginalizing over \mathcal{A}^X , this is only a null-set contribution; furthermore, the two hypotheses are still, by construction, *logically* exclusive. The same reasoning applies to $\tilde{\mathcal{H}}_{\text{tL}}^{X\ell}$. Hence, the probabilities of these three hypotheses must simply add up:

$$\begin{aligned} P\left(\hat{\mathcal{H}}_{\text{GLtL}} \middle| \mathbf{x}, \mathcal{I}\right) &= P\left(\hat{\mathcal{H}}_{\text{G}} \middle| \mathbf{x}, \mathcal{I}\right) + P\left(\hat{\mathcal{H}}_{\text{L}} \middle| \mathbf{x}, \mathcal{I}\right) \\ &\quad + P\left(\hat{\mathcal{H}}_{\text{tL}} \middle| \mathbf{x}, \mathcal{I}\right) \\ &= P\left(\hat{\mathcal{H}}_{\text{G}} \middle| \mathbf{x}, \mathcal{I}\right) \left(1 + \sum_{X=1}^{N_{\text{det}}} \tilde{\omega}_{\text{L/G}}^X e^{\hat{\mathcal{F}}^X - N_{\text{seg}} \mathcal{F}_*^{(0)}} \right. \\ &\quad \left. + \sum_{X\ell} \tilde{\omega}_{\text{tL/G}}^{X\ell} e^{\tilde{\mathcal{F}}^{X\ell} - \mathcal{F}_*^{(0)}} \right). \end{aligned} \quad (19)$$

Then, the odds ratio between the classical persistent-CW signal hypothesis $\hat{\mathcal{H}}_{\text{S}}$ and the combined triple-noise hypothesis $\hat{\mathcal{H}}_{\text{GLtL}}$ is

$$\begin{aligned} \hat{\mathcal{O}}_{\text{S/GLtL}} &= \hat{\mathcal{O}}_{\text{S/G}} e^{\hat{\mathcal{F}}} \bigg/ \left(e^{N_{\text{seg}} \mathcal{F}_*^{(0)}} + \sum_{X=1}^{N_{\text{det}}} \tilde{\omega}_{\text{L/G}}^X e^{\hat{\mathcal{F}}^X} \right. \\ &\quad \left. + \sum_{X\ell} \tilde{\omega}_{\text{tL/G}}^{X\ell} e^{\tilde{\mathcal{F}}^{X\ell} + (N_{\text{seg}} - 1) \mathcal{F}_*^{(0)}} \right), \end{aligned} \quad (20)$$

where, just as a reminder, the semicoherent $\hat{\mathcal{F}}$ -statistics are $\hat{\mathcal{F}} = \sum_{\ell} \tilde{\mathcal{F}}^{\ell}$ and $\hat{\mathcal{F}}^X = \sum_{\ell} \tilde{\mathcal{F}}^{X\ell}$.

With the total prior disturbance odds $\hat{\omega}_{\text{L/G}} \equiv \sum_X \hat{\omega}_{\text{L/G}}^X$ and $\hat{\omega}_{\text{tL/G}} \equiv \sum_{X\ell} \tilde{\omega}_{\text{tL/G}}^{X\ell}$, we introduce the following shorthands for prior probabilities conditional on the composite noise hypothesis $\hat{\mathcal{H}}_{\text{GLtL}}$, generalizing the \hat{p}_{L} and \hat{p}_{L}^X from Eq. (12):

$$\hat{p}_{\text{L}}^X \equiv P\left(\mathcal{H}_{\text{L}}^X \middle| \hat{\mathcal{H}}_{\text{GLtL}}, \mathcal{I}\right) = \frac{\hat{\omega}_{\text{L/G}}^X}{1 + \hat{\omega}_{\text{L/G}} + \hat{\omega}_{\text{tL/G}}}, \quad (21a)$$

$$\tilde{\hat{p}}_{\text{tL}}^{X\ell} \equiv P\left(\tilde{\mathcal{H}}_{\text{tL}}^{X\ell} \middle| \hat{\mathcal{H}}_{\text{GLtL}}, \mathcal{I}\right) = \frac{\tilde{\omega}_{\text{tL/G}}^{X\ell}}{1 + \hat{\omega}_{\text{L/G}} + \hat{\omega}_{\text{tL/G}}}, \quad (21b)$$

$$\hat{p}_{\text{LtL}} \equiv P\left(\hat{\mathcal{H}}_{\text{LtL}} \middle| \hat{\mathcal{H}}_{\text{GLtL}}, \mathcal{I}\right) = \frac{\hat{\omega}_{\text{LtL/G}}}{1 + \hat{\omega}_{\text{LtL/G}}}. \quad (21c)$$

This allows us to write the corresponding Bayes factor as

$$\widehat{B}_{S/GLtL} = \frac{e^{\widehat{\mathcal{F}}}}{(1 - \widehat{p}_{LtL}) e^{N_{\text{seg}} \mathcal{F}_*^{(0)}} + \sum_X \widehat{p}_L^X e^{\widehat{\mathcal{F}}^X} + \sum_{X\ell} \widetilde{p}_{tL}^{X\ell} e^{\widehat{\mathcal{F}}^{X\ell} + (N_{\text{seg}} - 1) \mathcal{F}_*^{(0)}}}. \quad (22)$$

We see that the difference between (i) the persistent-line term already present in the $\widehat{B}_{S/GL}$ of Ref. (13) and (ii) the newly-introduced transient-line term is that we have either (i) a sum over X of the exponentials of a sum over ℓ of $\widetilde{\mathcal{F}}^{X\ell}$, or (ii) a double sum over X and ℓ of the exponentials of each individual $\widetilde{\mathcal{F}}^{X\ell}$ plus a large constant term $(N_{\text{seg}} - 1) \mathcal{F}_*^{(0)}$.

Hence, if there is a strong disturbance in a single (X, ℓ) combination and if the transition-scale parameter $\mathcal{F}_*^{(0)}$ has been chosen as higher than the typical $\widetilde{\mathcal{F}}^{X\ell}$ in pure Gaussian noise (in accordance with the tuning procedure described in section VI.B of Paper I), then the latter term can dominate in the denominator. This will make $\widehat{B}_{S/GLtL}$ stricter in suppressing these transient disturbances than $\widehat{B}_{S/GL}$.

We could have introduced an additional free tuning parameter into $\widehat{B}_{S/GLtL}$ by using a different cutoff on the $\mathcal{A}^{X\ell}$ prior in $\widehat{\mathcal{H}}_{tL}^{X\ell}$ than for the \mathcal{A}^X in $\widehat{\mathcal{H}}_L^X$, resulting in a different $\mathcal{F}_*^{(0)'$ appearing. However, we already have freedom in the relative weights of persistent and transient line contributions through the \widehat{p}_L^X and $\widetilde{p}_{tL}^{X\ell}$, and there is no clear physical motivation in such a complication of the amplitude priors (which were chosen ad-hoc, to reproduce the \mathcal{F} -statistic, in the first place, cf. Refs. [27, 39]). Hence, we refrain from this possibility, and use the tests in Sec. V to demonstrate sufficient flexibility of $\widehat{B}_{S/GLtL}$ without it.

As the denominator of $\widehat{B}_{S/GLtL}$ is a sum of exponentials (or weighted exponentials, but of course the log of the weights can be absorbed into the exponents), it is often dominated by a single term. The same is true for $B_{S/GL}$, and its limiting behavior in various cases was discussed in Sec. IV.B1 of Paper I. Here, we just give an expression for $\ln \widehat{B}_{S/GLtL}$ written as a sum of the dominant term and a logarithmic correction:

$$\ln \widehat{B}_{S/GLtL} = \mathcal{F} - D_{\text{max}} - \ln \left(\sum_{D \in \mathcal{D}} e^{D - D_{\text{max}}} \right), \quad (23)$$

where $D_{\text{max}} \equiv \max \mathcal{D}$ is the maximum of the set of denominator exponents

$$\mathcal{D} \equiv \left\{ N_{\text{seg}} \mathcal{F}_*^{(0)} + \ln(1 - \widehat{p}_{LtL}), \mathcal{F}^X + \ln \widehat{p}_L^X, \right. \\ \left. \widetilde{\mathcal{F}}^{X\ell} + (N_{\text{seg}} - 1) \mathcal{F}_*^{(0)} + \ln \widetilde{p}_{tL}^{X\ell} \right\}. \quad (24)$$

In computer implementations, this form is useful both for numerical stability (avoiding underflows) and to speed up computation when the correction term can be neglected, $\ln \widehat{B}_{S/GLtL} \approx \mathcal{F} - D_{\text{max}}$.

We also consider an intermediate step where we reduce the the $\sum_{X\ell}$ -sum in the denominator to the highest per-segment contributions from each detector, but keep all other terms. This will reduce computational cost while also corresponding to the initial assumption of a single-segment disturbance: again, because of the exponentials, a single significantly increased $\widetilde{\mathcal{F}}^{X\ell}$ will easily dominate over all others. Hence, in many cases a good approximation to the Bayes factor will be given by

$$\widehat{B}_{S/GLtL} \approx e^{\widehat{\mathcal{F}}} / \left((1 - \widehat{p}_{LtL}) e^{N_{\text{seg}} \mathcal{F}_*^{(0)}} \right. \\ \left. + \sum_X \widehat{p}_L^X e^{\widehat{\mathcal{F}}^X} + \sum_X \widetilde{p}_{tL}^{X\mu(X)} e^{\widetilde{\mathcal{F}}^{X\mu(X)} + (N_{\text{seg}} - 1) \mathcal{F}_*^{(0)}} \right), \quad (25)$$

where $\mu(X)$ is the segment number for which $\widetilde{p}_{tL}^{X\mu(X)} e^{\widetilde{\mathcal{F}}^{X\mu(X)}} \equiv \max_{\ell} \left(\widetilde{p}_{tL}^{X\ell} e^{\widetilde{\mathcal{F}}^{X\ell}} \right)$.

In practice, it can be easier to further simplify the search code by only returning single-segment information for the segment m with the highest *multi-detector* $\widetilde{\mathcal{F}}^m \equiv \max_{\ell} \widetilde{\mathcal{F}}^{\ell}$. Hence, we define an ad-hoc modified ‘loudest-only’ detection statistic

$$\widehat{B}_{S/GLtL,lo} \equiv e^{\widehat{\mathcal{F}}} / \left((1 - \widehat{p}_{LtL}) e^{N_{\text{seg}} \mathcal{F}_*^{(0)}} \right. \\ \left. + \sum_{X=1}^{N_{\text{det}}} \widehat{p}_L^X e^{\widehat{\mathcal{F}}^X} + \sum_{X=1}^{N_{\text{det}}} \widetilde{p}_{tL}^{Xm} e^{\widetilde{\mathcal{F}}^{Xm} + (N_{\text{seg}} - 1) \mathcal{F}_*^{(0)}} \right). \quad (26)$$

This quantity could, in principle, differ quite significantly from the actual Bayes factor $\widehat{B}_{S/GLtL}$, so we will test its efficiency as a detection statistic in Sec. V.

IV. GENERAL DETECTION STATISTIC FOR PERSISTENT OR TRANSIENT SIGNALS, ROBUST TO PERSISTENT OR TRANSIENT SINGLE-DETECTOR LINES

CW-like transient signals might be interesting search targets. [27, 28, 34] One might now anticipate that $\widehat{B}_{S/GLtL}$ is *too restrictive* towards these, as a multi-detector-coherent signal in a single segment can increase the denominator of Eq. (22) more than the numerator.

However, the approach of considering more general hypotheses built up from the set $\{\widetilde{\mathcal{F}}^{\ell}, \{\widetilde{\mathcal{F}}^{X\ell}\}\}$ should actually allow for *more sensitivity* towards transient signals than any detection statistic based only on the total semi-coherent results, like $\widehat{\mathcal{F}}$ and $\widehat{O}_{S/GL}$.

So we now try to improve over $\widehat{B}_{S/GLtL}$ by considering a generalized detection statistic, answering the following

question: how likely is *any type of CW-like signal* (persistent or transient), in comparison with either Gaussian noise, a persistent line or a transient line?

Starting from the full set of single-segment $\{\tilde{\mathcal{F}}^\ell, \{\tilde{\mathcal{F}}^{X\ell}\}\}$, the most general answer would involve a large set of hypotheses for signals in different numbers of segments. But here we keep to the simplifying assumption of single-segment transients, introducing a transient-signal hypothesis as the multi-detector version of Eq. (14):

$$\tilde{\mathcal{H}}_{\text{tS}}^\ell : \mathbf{x}^\ell(t) = \mathbf{n}^\ell(t) + \mathbf{h}^\ell(t; \mathcal{A}^\ell). \quad (27)$$

Note that this is different from the single-segment, single-detector transient-line hypothesis $\tilde{\mathcal{H}}_{\text{tL}}^{X\ell}$ from Eq. (14) only if the data set for segment ℓ contains data for at least two detectors X . In this section, we assume this to be the case for the whole data set. However, in the real world the components of a multi-detector network often have different duty factors and standard data selection methods [44] can result in segments with data from one detector only, or with negligible amounts of data from the other detectors.

We will test the robustness of our detection statistic, derived with the assumption of full segment coverage by all detectors, for a data set with realistic duty factors in Sec. V, and discuss ways to deal with the slight issues it can cause, in Sec. V C.

Let us continue from the posterior distribution for $\tilde{\mathcal{H}}_{\text{tS}}^\ell$, which is analogous to Eq. (15):

$$P\left(\tilde{\mathcal{H}}_{\text{tS}}^\ell \mid \mathbf{x}^\ell, \mathcal{I}\right) = P\left(\tilde{\mathcal{H}}_{\text{G}}^\ell \mid \mathbf{x}^\ell, \mathcal{I}\right) \tilde{o}_{\text{tS/G}}^\ell e^{\tilde{\mathcal{F}}^\ell(\mathbf{x}^\ell) - \mathcal{F}_*^{(0)}}. \quad (28)$$

The hypothesis $\hat{\mathcal{H}}_{\text{tS}}$ for a transient signal in an arbitrary segment is the OR-combination of $\tilde{\mathcal{H}}_{\text{tS}}^\ell$ analogous to Eq. (16), so that the posterior $P\left(\hat{\mathcal{H}}_{\text{tS}} \mid \mathbf{x}, \mathcal{I}\right)$ is obtained

$$\hat{B}_{\text{StS/GLtL}} = \frac{(1 - \tilde{p}_{\text{tS}}) e^{\hat{\mathcal{F}}} + \sum_{\ell} \tilde{p}_{\text{tS}}^\ell e^{\tilde{\mathcal{F}}^\ell + (N_{\text{seg}} - 1)\mathcal{F}_*^{(0)}}}{(1 - \hat{p}_{\text{LtL}}) e^{N_{\text{seg}}\mathcal{F}_*^{(0)}} + \sum_X \hat{p}_{\text{L}}^X e^{\hat{\mathcal{F}}^X} + \sum_{X\ell} \hat{p}_{\text{tL}}^{X\ell} e^{\tilde{\mathcal{F}}^{X\ell} + (N_{\text{seg}} - 1)\mathcal{F}_*^{(0)}}}. \quad (34)$$

As was the case for $\hat{B}_{\text{S/GLtL}}$ from Eq. (22), additional freedom in tuning this statistic could be obtained from different amplitude-prior cutoffs in $\hat{\mathcal{H}}_{\text{L}}$, $\hat{\mathcal{H}}_{\text{tL}}$ and now also $\hat{\mathcal{H}}_{\text{S}}$ and $\hat{\mathcal{H}}_{\text{tS}}$. But again we restrict ourselves to using the same cutoff, resulting in a single tuning parameter $\mathcal{F}_*^{(0)}$,

in analogy with Eq. (17):

$$\begin{aligned} P\left(\hat{\mathcal{H}}_{\text{tS}} \mid \mathbf{x}, \mathcal{I}\right) &= \sum_{\ell=1}^{N_{\text{seg}}} P\left(\tilde{\mathcal{H}}_{\text{tS}}^\ell \mid \mathbf{x}^\ell, \mathcal{I}\right) \prod_{\ell' \neq \ell} P\left(\tilde{\mathcal{H}}_{\text{G}}^{\ell'} \mid \mathbf{x}^{\ell'}, \mathcal{I}\right) \\ &= P\left(\hat{\mathcal{H}}_{\text{G}} \mid \mathbf{x}, \mathcal{I}\right) \sum_{\ell=1}^{N_{\text{seg}}} \tilde{o}_{\text{tS/G}}^\ell e^{\tilde{\mathcal{F}}^\ell - \mathcal{F}_*^{(0)}}. \end{aligned} \quad (29)$$

As before for the various noise hypotheses, the probabilities for the persistent-signal hypothesis \mathcal{H}_{S} and $\hat{\mathcal{H}}_{\text{tS}}$ add up to that of a more general persistent-or-transient ‘CW-like’ signal:

$$\begin{aligned} P\left(\hat{\mathcal{H}}_{\text{StS}} \mid \mathbf{x}, \mathcal{I}\right) &= P\left(\hat{\mathcal{H}}_{\text{S}} \mid \mathbf{x}, \mathcal{I}\right) + P\left(\hat{\mathcal{H}}_{\text{tS}} \mid \mathbf{x}, \mathcal{I}\right) \quad (30) \\ &= P\left(\hat{\mathcal{H}}_{\text{G}} \mid \mathbf{x}, \mathcal{I}\right) \left(\hat{o}_{\text{S/G}} e^{\hat{\mathcal{F}} - N_{\text{seg}}\mathcal{F}_*^{(0)}} + \sum_{\ell=1}^{N_{\text{seg}}} \tilde{o}_{\text{tS/G}}^\ell e^{\tilde{\mathcal{F}}^\ell - \mathcal{F}_*^{(0)}} \right). \end{aligned}$$

The odds ratio between generalized signal hypothesis and generalized noise hypothesis is then

$$\begin{aligned} \hat{O}_{\text{StS/GLtL}} &= \left(\hat{o}_{\text{S/G}} e^{\hat{\mathcal{F}}} + \sum_{\ell} \tilde{o}_{\text{tS/G}}^\ell e^{\tilde{\mathcal{F}}^\ell + (N_{\text{seg}} - 1)\mathcal{F}_*^{(0)}} \right) \quad (31) \\ &\left/ \left(e^{N_{\text{seg}}\mathcal{F}_*^{(0)}} + \sum_X \hat{o}_{\text{L/G}}^X e^{\hat{\mathcal{F}}^X} + \sum_{X\ell} \tilde{o}_{\text{tL/G}}^{X\ell} e^{\tilde{\mathcal{F}}^{X\ell} + (N_{\text{seg}} - 1)\mathcal{F}_*^{(0)}} \right). \end{aligned}$$

Introducing additional prior-weight variables in analogy to \hat{p}_{L}^X , $\tilde{p}_{\text{tL}}^{X\ell}$ from Eq. (21):

$$\begin{aligned} \hat{p}_{\text{S}} &\equiv P\left(\mathcal{H}_{\text{S}} \mid \hat{\mathcal{H}}_{\text{StS}}, \mathcal{I}\right) = \frac{\hat{o}_{\text{S/G}}}{\hat{o}_{\text{S/G}} + \hat{o}_{\text{tS/G}}} \quad (32) \\ &= (1 - \tilde{p}_{\text{tS}}) = \left(1 - \sum_{\ell=1}^{N_{\text{seg}}} \tilde{p}_{\text{tS}}^\ell \right), \end{aligned}$$

$$\tilde{p}_{\text{tS}}^\ell \equiv P\left(\tilde{\mathcal{H}}_{\text{tS}}^\ell \mid \hat{\mathcal{H}}_{\text{StS}}, \mathcal{I}\right) = \frac{\tilde{o}_{\text{tS/G}}^\ell}{\hat{o}_{\text{S/G}} + \hat{o}_{\text{tS/G}}}, \quad (33)$$

we obtain the Bayes factor as

and use only the set of prior variables $\{\hat{p}_{\text{S}}, \tilde{p}_{\text{tS}}^\ell, \hat{p}_{\text{LtL}}, \tilde{p}_{\text{tL}}^{X\ell}\}$ to weight between the various contributions.

Next, we consider the logarithm of this Bayes factor, splitting numerator and denominator separately into sums of a dominant term and a logarithmic correction,

which generalizes Eq. (23):

$$\ln \widehat{B}_{S/GLtL} = E_{\max} + \ln \left(\sum_{E \in \mathcal{E}} e^{E - E_{\max}} \right) - D_{\max} - \ln \left(\sum_{D \in \mathcal{D}} e^{D - D_{\max}} \right), \quad (35)$$

where D_{\max} is the maximum of the same set of denominator exponents given in Eq. (24) and $E_{\max} = \max \mathcal{E}$ is the maximum of the numerator exponents:

$$\mathcal{E} = \left\{ \mathcal{F} + \ln \widehat{p}_S, \widetilde{\mathcal{F}}^\ell + (N_{\text{seg}} - 1) \mathcal{F}_*^{(0)} + \ln \widetilde{p}_{tS}^\ell \right\}. \quad (36)$$

Again, for transient signals and disturbances that are indeed limited to a single segment (or reasonably close to being so), it should suffice to compute an approximate Bayes factor using only the maximum single-segment contributions:

$$\widehat{B}_{StS/GLtL} \approx \left(\widehat{p}_S e^{\widehat{\mathcal{F}}} + \widetilde{p}_{tS}^\mu e^{\widetilde{\mathcal{F}}^\mu + (N_{\text{seg}} - 1) \mathcal{F}_*^{(0)}} \right) / \left(\left((1 - \widehat{p}_{LtL}) e^{N_{\text{seg}} \mathcal{F}_*^{(0)}} + \sum_X \widehat{p}_L^X e^{\widehat{\mathcal{F}}^X} + \sum_X \widetilde{p}_{tL}^{X\mu(X)} e^{\widetilde{\mathcal{F}}^{X\mu(X)} + (N_{\text{seg}} - 1) \mathcal{F}_*^{(0)}} \right) \right), \quad (37)$$

where μ is the segment number for which $\widetilde{p}_{tS}^\mu e^{\widetilde{\mathcal{F}}^\mu} \equiv \max_\ell \left(\widetilde{p}_{tS}^\ell e^{\widetilde{\mathcal{F}}^\ell} \right)$ and $\mu(X)$ is the segment number for which $\widetilde{p}_{tL}^{X\mu(X)} e^{\widetilde{\mathcal{F}}^{X\mu(X)}} \equiv \max_\ell \left(\widetilde{p}_{tL}^{X\ell} e^{\widetilde{\mathcal{F}}^{X\ell}} \right)$.

As in Eq. (26), we also define an ad-hoc modified ‘loudest-only’ detection statistic where we use only information from one segment m with the highest *multi-detector* $\widetilde{\mathcal{F}}^m \equiv \max_\ell \widetilde{\mathcal{F}}^\ell$, and which we will test in Sec. V:

$$\widehat{B}_{StS/GLtL,lo} \equiv \left(\widehat{p}_S e^{\widehat{\mathcal{F}}} + \widetilde{p}_{tS}^m e^{\widetilde{\mathcal{F}}^m + (N_{\text{seg}} - 1) \mathcal{F}_*^{(0)}} \right) / \left(\left((1 - \widehat{p}_{LtL}) e^{N_{\text{seg}} \mathcal{F}_*^{(0)}} + \sum_X \widehat{p}_L^X e^{\widehat{\mathcal{F}}^X} + \sum_X \widetilde{p}_{tL}^{Xm} e^{\widetilde{\mathcal{F}}^{Xm} + (N_{\text{seg}} - 1) \mathcal{F}_*^{(0)}} \right) \right). \quad (38)$$

These expressions also simplify significantly if all $\widehat{o}_{tS/G}^\ell = \widehat{o}_{S/G}$ and $\widehat{o}_{tL/G}^{X\ell} = \widehat{o}_{L/G}^X$, which we will assume for most of the test cases in the next section.

V. TESTS ON SIMULATED DATA

In this section, we present some tests of the new Bayes factors $\widehat{B}_{S/GLtL}$ and $\widehat{B}_{StS/GLtL}$ in the form of injection studies on simulated data, where simulated CW and tCW signals (‘injections’) are recovered from simulated noise. We use the same basic procedure as described in section VII.B of Paper I,

A. Search setup and data sets

For two reasons, it is important to test these detection statistics with realistic data and a search setup that is close to what is used in practice: First, the approach in this paper is to provide a simple extension of the established $\widehat{\mathcal{F}}$ -statistics and line-robust statistics search codes, which should be directly applicable in current search efforts. Second, as we are interested in time-domain features, the characteristics of real data sets will be important for any performance demonstration, especially the occurrence of gaps in the data.

Hence, we use fully simulated data, but with realistic duty factors taken from the real LIGO S6 data. One data set contains pure Gaussian noise, whereas an additional transient disturbance is present in the second data set. We have also tested, on a third data set with a persistent line, that the new Bayes factors $\widehat{B}_{S/GLtL}$ and $\widehat{B}_{StS/GLtL}$ at least reproduce the detection efficiency of $B_{S/GL}$. To avoid redundancy with Ref. [36], that set of results is not shown and discussed in detail here.

1. Search setup

Our search setup mimics the Einstein@Home [45] ‘S6Bucket’ search [46] on LIGO S6 data: we use data spanning about 255 d, analyzed semicoherently with $N_{\text{seg}} = 90$ segments of $T_{\text{seg}} = 60$ h.

The analysis is performed with the `HierarchSearchGCT` code [47], a semicoherent Stack-Slide implementation based on the *global correlations transform* method of Ref. [11]. We use the same search grids as the ‘S6Bucket’ search. `HierarchSearchGCT` refines the search grid in the spindown parameter \dot{f} (by a factor γ_r), but not over the sky. It returns a *toplist* of the most significant candidates ranked by a chosen semicoherent statistic ($\widehat{\mathcal{F}}$ or $B_{S/GL}$). For this study, we have modified this code to also return the single-segment $\widetilde{\mathcal{F}}^\ell$ -statistics for each toplist candidate.

We first analyze a 50 mHz band of each simulated noise-only data set (purely Gaussian and Gaussian + transient disturbance), and obtain the maximum of each detection statistic over the whole sky and f, \dot{f} range.

Then, for a set of fixed signal strengths h_0 , CW or tCW signals with otherwise random parameters are injected into the same noise realization, and searched for again over a smaller *search-box*, which is a subset of the original search grid containing (but usually not centered on) the injection point. A signal is considered detected if the highest value from this search-box exceeds the maximum value from the pure-noise search.

The search parameters for both the full-band noise-only search and for the smaller injection search-boxes are given in Table I.

Another point where we construct our procedure in analogy with the ‘S6Bucket’ search is the ranking of candidates in the toplist kept by the `HierarchSearchGCT` code. For each search job (51 sky partitions per noise-

common search parameters	
detectors	LIGO H1, L1
t_{start} [s]	949469977
t_{end} [s]	971529850
$N_{\text{seg}}, N_{\text{seg}}^{\text{H1}}, N_{\text{seg}}^{\text{L1}}$	90, 89, 90
T_{seg}	60h
frequency resolution δf	$\approx 1.6143 \cdot 10^{-6}$ Hz
spindown resolution $\delta \dot{f}$	$\approx 5.7890 \cdot 10^{-11}$ Hz ²
\dot{f} refinement factor γ_r	230
nominal sky-grid mismatch	0.3
original toplists	$\hat{\mathcal{F}}$ and $B_{\text{S/L}}(o_{\text{L/G}}^X = 1.0)$
toplist length	1000
full-band search parameters	
min f	50.0 Hz
frequency range Δf	0.05 Hz
min \dot{f}	$\approx -2.6425 \cdot 10^{-9}$ Hz ²
spindown range $\Delta \dot{f}$	$\approx 2.9067 \cdot 10^{-9}$ Hz ²
sky points N_{sky}	707
search jobs (sky partitions)	51
injection search-box	
\dot{f} range	0.001 Hz
f range	$\approx 2.3156 \cdot 10^{-10}$ Hz ² (4 coarse-grid points)
sky points	10

TABLE I. Search parameters for pure-noise (‘full-band’) and per-injection searches with `lalapps_HierarchSearchGCT`.

only search, or one search-box per injection) we keep two toplists with 1000 candidates each. One toplist is sorted by $\hat{\mathcal{F}}$ and one by the pure line-veto statistic $B_{\text{S/L}}(o_{\text{L/G}}^X = 1.0)$, which corresponds to $B_{\text{S/GL}}$ in the limit of $\mathcal{F}_*^{(0)} \rightarrow -\infty$. All other detection statistics are then computed from the *union* of these two toplists.

In principle, this procedure could lead to some noise outliers or some injections being missed for the ‘recomputed’ statistics. However, the two toplists (classic $\hat{\mathcal{F}}$ -statistic and ‘pure line-veto statistic’) are very ‘orthogonal’ in the sense that one is nearly optimal for Gaussian data and one is tuned towards strong disturbances, so that candidates that would be significant by one of the other Bayes factors are very likely to appear in at least one of these two toplists. Also, tests with longer toplists have found that this approach is generally sufficient to not lose any would-be high-significance candidates of any recomputed statistic by having them below the threshold of both ranking statistics.

2. Simulated data sets

To generate our data, we used the duty factors of the H1 and L1 detectors for the data selection of the Einstein@Home ‘S6Bucket’ search on LIGO S6 data: this gives us 6156 SFTs in H1 and 5924 SFTs in L1, each SFT 1800 s long, with realistic gaps in-between.

The data selection method [44] used to generate the ‘S6Bucket’ segment list was optimized for total sensitiv-

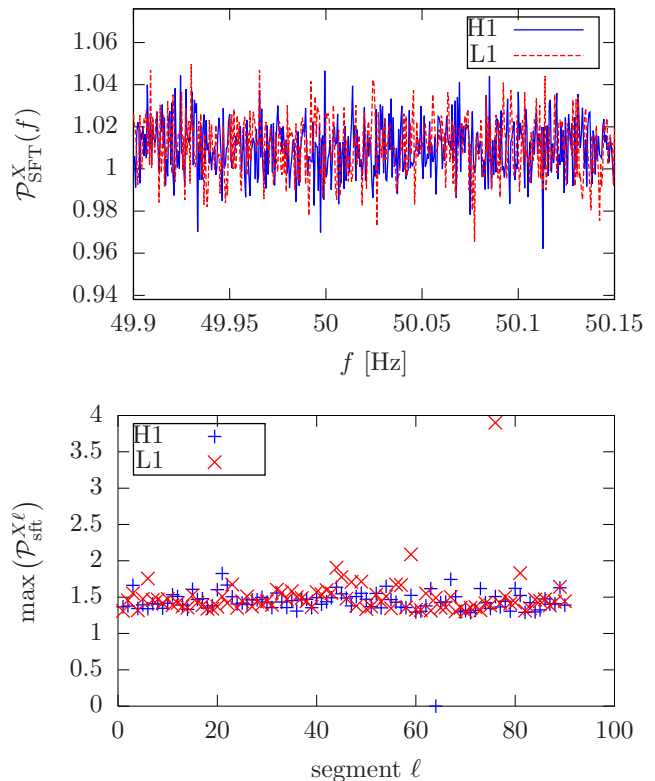


FIG. 1. Pure Gaussian noise data set. Top panel: Normalized SFT power $\mathcal{P}_{\text{SFT}}^X$ averaged over all $N_{\text{seg}} = 90$ segments. Bottom panel: Single-segment $\max_f \mathcal{P}_{\text{SFT}}^{X\ell}$, maximized over SFT frequency bins, as a function of segments ℓ .

ity and did not ensure uniform duty factors over segments and detectors. Hence, it happens to have two particularly unequal segments, where one detector contributes no or very little data (compared to an average of 67 SFTs per segment and detectors): segment 64 (of 90) has no data from detector H1, and segment 76 has only 4 SFTs from detector L1.

The first ‘quiet’ data set is pure simulated Gaussian noise, from the `Makefakedata_v5` code [47], with the sensitivity of the two detectors being realistically slightly unequal: the single-sided power-spectral densities (PSD) are $\sqrt{S^{\text{H1}}} = 3.2591 \cdot 10^{-22}$ Hz^{-1/2} and $\sqrt{S^{\text{L1}}} = 2.9182 \cdot 10^{-22}$ Hz^{-1/2}.

The per-detector normalized SFT power

$$\mathcal{P}_{\text{SFT}}^X(f) \equiv \frac{2}{N_{\text{SFT}} T_{\text{SFT}}} \sum_{\alpha=1}^{N_{\text{SFT}}} \frac{|\tilde{x}_{\alpha}^X(f)|^2}{S_{\alpha}^X(f)} \quad (39)$$

for this data set is shown in Fig. 1, both as a frequency-dependent average $\mathcal{P}_{\text{SFT}}^X(f)$ over the whole data set and in the form of a single-segment maximum $\max_f \mathcal{P}_{\text{SFT}}^{X\ell}$ over SFT frequency bins, as a function of segments ℓ . The apparent outlier $\max_f \mathcal{P}_{\text{SFT}}^{\text{L1}\ell=76} \approx 3.9$ is just an effect of low-number statistics, as segment 76 contains only 4 SFTs

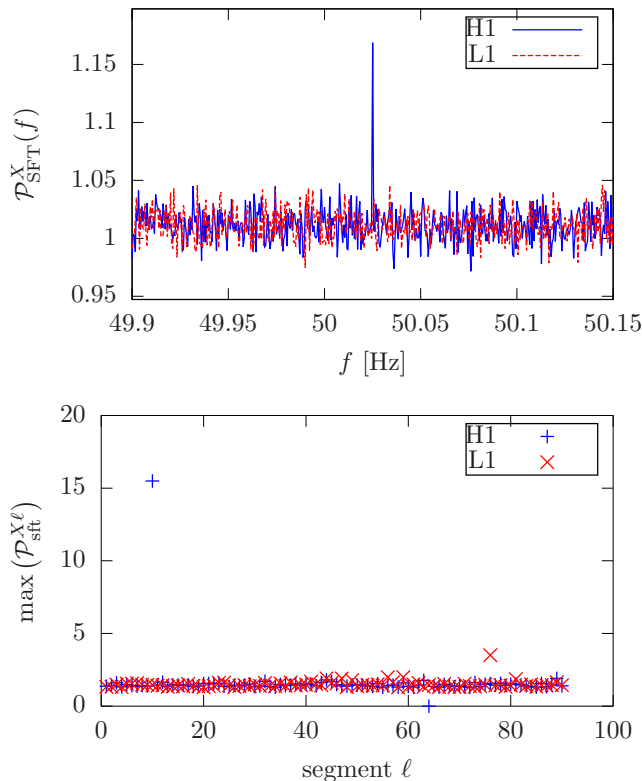


FIG. 2. Data set with Gaussian noise and a single-detector stationary line injected for the duration of segment $\ell = 10$ in detector H1. Panels are the same as in Fig. 1.

from detector L1.

We have also generated a second data set containing a transient single-detector disturbance. We started with an independent realization of Gaussian noise with the same timestamps and PSDs as the first set, and then used `Makefakedata_v4` [47] to inject a stationary line feature with fixed amplitude $h_{0L} = 4 \cdot 10^{-23}$ and frequency $f_L = 50.025$ Hz in a single detector (H1) during a single segment $\ell_L = 10$. (As of writing this paper, the newer `MFD_v5` code did not support stationary line injections.)

The normalized SFT power for this data set is shown in Fig. 2. We see that the disturbance produces a very high single-segment $\max_f \mathcal{P}_{\text{SFT}}^{\text{H1}\ell=10} \approx 15$. It is also strong

enough to show up in the average $\mathcal{P}_{\text{SFT}}^X(f)$ over the whole data set, but in this average it is much weaker than the persistent lines studied before (cf. Fig. 7 of Paper I).

This simulated disturbance is similar to a family of transient disturbances in LIGO S6 data informally called ‘pizza-slice disturbances’ due to their shape in 3D plots of $\widehat{\mathcal{F}}$ -statistics against frequency f and spin-down \dot{f} . [23] Fig. 3 presents such a plot for our simulated data set. Though a sharp line in $\mathcal{P}_{\text{SFT}}^X$, the semicoherent search sees this transient disturbance as a wide structure in parameter space. Different templates match the disturbance at different times, leading to the ‘pizza-slice’ shape.

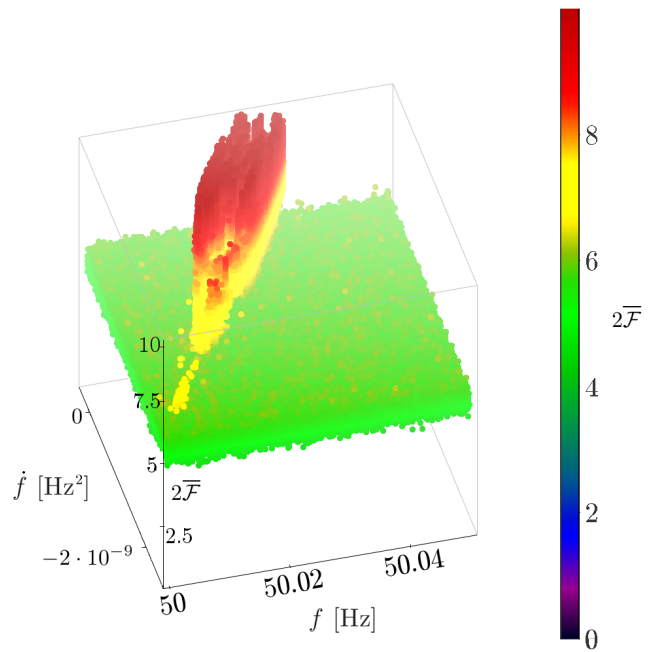


FIG. 3. Data set with Gaussian noise and a single-detector stationary line injected for the duration of segment $\ell = 10$ in detector H1. The figure shows the average multi-detector semicoherent $2\overline{\mathcal{F}}$ -statistic, over 90 segments, with the ‘full-band’ search parameters listed in Table I, as a function of frequency f and spindown \dot{f} .

The simulation result is somewhat narrower than the typical LIGO S6 ‘pizza slice’, since its duration is a whole segment of $T_{\text{seg}} = 60$ h, while the corresponding disturbances in S6 data typically last only for a few SFTs.

In all test cases, 1000 signals are injected per h_0 value, with random amplitude parameters $\cos \iota$, ϕ_0 , Ψ and with f , \dot{f} and sky position randomly distributed over the full search range as given in Table I.

3. Tuning the free parameters of the line-robust statistics

A global value for the transition-scale parameter $\mathcal{F}_*^{(0)}$ is determined through requiring *safety* in quiet data, choosing the minimum value required to have negligible differences in detection probability to the $\widehat{\mathcal{F}}$ -statistic. This statement holds down to the false-alarm level probed by this study, which is bounded by the inverse number of fine-grid templates ($N_{\text{templ}} = \gamma_r N_{\text{sky}} \frac{\Delta f}{\delta f} \frac{\Delta \dot{f}}{\delta \dot{f}} \approx 2.3 \cdot 10^{11}$) in the search setup, but will effectively be somewhat higher due to template overlap.

For the original $\widehat{B}_{\text{S/GL}}$, we use a value of $\mathcal{F}_*^{(0)} \approx 3.027$ found in more extensive studies on LIGO S6 data [46]. For $\widehat{B}_{\text{S/GLtL}}$ and $\widehat{B}_{\text{StS/GLtL}}$ the present injection study on the pure Gaussian-noise data set leads us to adopt $\mathcal{F}_*^{(0)} \approx 3.0$, though possibly an optimal value might be slightly higher: we only checked steps of 0.1 in $\mathcal{F}_*^{(0)}$.

For the per-detector line-priors, we use

$\hat{o}_{L/G}^X = \tilde{o}_{L/G}^{X\ell} = 0.001$ for all X and ℓ in both data sets, corresponding to the conservative lower truncation suggested in section VI.A of Paper I.

However, we will also investigate the effect of setting $\tilde{o}_{L/G}^{X\ell=64,76} = 0.0$ in the two segments with no or small contributions from one of the two detectors. The rationale for this modification is that the single-segment signal hypothesis $\tilde{\mathcal{H}}_{tS}^\ell$ of Eq. (27) becomes indistinguishable from our transient-line hypothesis $\tilde{\mathcal{H}}_{tL}^{X\ell}$ of Eq. (14) when that segment is completely dominated by a single detector.

B. persistent CW signals

For persistent CW signals, the injection procedure is identical to that in Paper I. Fig. 4 shows results in the form of detection probabilities p_{det} for the various statistics as functions of the scaled signal amplitude h_0/\sqrt{S} .

As discussed in the previous paragraph, tuning $\mathcal{F}_*^{(0)} = 3$ allows both $\hat{B}_{S/GLtL}$ and $\hat{B}_{StS/GLtL}$ to match almost perfectly the detection efficiency of the $\hat{\mathcal{F}}$ -statistic and of $\hat{B}_{S/GL}$ in quiet Gaussian data, with maximum discrepancies in p_{det} of 1% (down to the false-alarm level of this search setup). These are smaller than the statistical uncertainties from 1000 injections, and could be resolved with a more detailed $\mathcal{F}_*^{(0)}$ tuning. In this case, all statistics reach 90% detection probability at $h_0^{90\%}/\sqrt{S} \approx 0.023$.

In the data set with a transient line-like single-detector disturbance, $\hat{\mathcal{F}}$ performs much worse, while $\hat{B}_{S/GL}$ loses a few % of p_{det} at any given h_0 . Here, the new $\hat{B}_{S/GLtL}$ performs best with no degradation from the quiet case, still achieving $h_0^{90\%}/\sqrt{S} \approx 0.023$. Taking into account the possibility of tCW signals (which are not actually present in this case), $\hat{B}_{StS/GLtL}$ only sacrifices about 1% in p_{det} , and still improves significantly over $\hat{B}_{S/GL}$.

In both cases, using the simplified ‘loudest-only’ detection statistics from Eqs. (26) and (38) with only one set of single-segment $\{\tilde{\mathcal{F}}^m, \{\tilde{\mathcal{F}}^{Xm}\}\}$ values (with m chosen so that $\tilde{\mathcal{F}}^m = \max_{\ell} \tilde{\mathcal{F}}^\ell$) does not decrease detection efficiency. No extra curves are plotted for these statistics.

Also, we see that the performance of the permanence veto [19–21] in the absence of tCW signals is closely reproduced by our new Bayes factors.

C. tCW signals of exactly one segment length

For the first set of transient signal injections, we simulate CW-like signals that are active during exactly one segment, i.e. with fixed $T_{\text{inj}} = T_{\text{seg}} = 60\text{h}$ and a start time corresponding to that of a randomly picked segment for each injection. Detection probabilities for this case are shown in Fig. 5, over both noise data sets (purely Gaussian and Gaussian + transient disturbance).

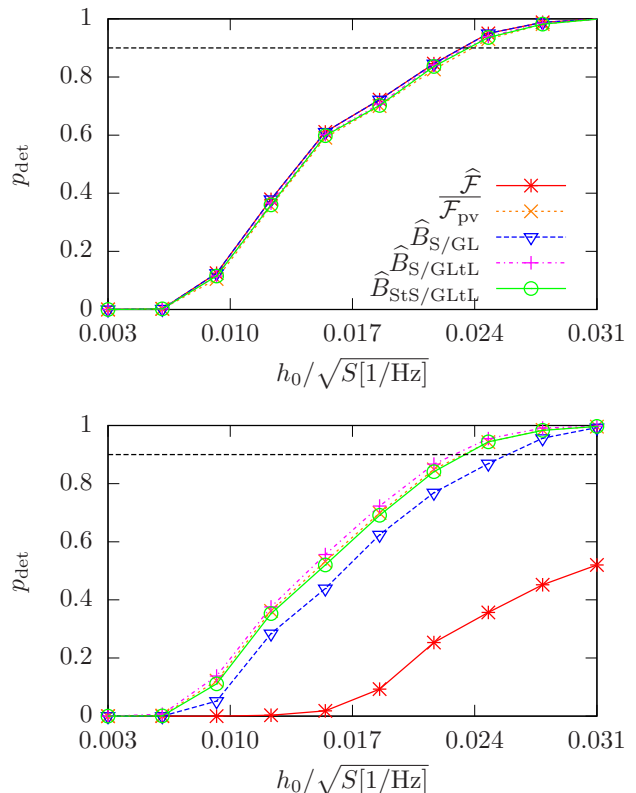


FIG. 4. Detection efficiency p_{det} for persistent CW signals, as a function of scaled signal amplitude h_0/\sqrt{S} , for the following semicoherent statistics: $\hat{\mathcal{F}}$, \mathcal{F}_{pv} (permanence veto), $\hat{B}_{S/GL}$ from Eq. (13), $\hat{B}_{S/GLtL}$ from Eq. (22), $\hat{B}_{StS/GLtL}$ from Eq. (34). The dashed horizontal lines marks $p_{\text{det}} = 90\%$. Top panel: injections in pure Gaussian noise, bottom panel: injections in Gaussian noise with a transient disturbance. Statistical uncertainties are smaller than the plot markers.

The established semicoherent detection statistics $\hat{\mathcal{F}}$ and $\hat{B}_{S/GL}$ achieve $h_0^{90\%}/\sqrt{S} \approx 0.1$ in the first, quiet data set. This is about a factor 4–5 worse than for persistent signals, which is actually already a smaller ratio than expected from the naive $\sqrt{T_{\text{obs}}/T_{\text{inj}}} = \sqrt{N_{\text{seg}}}$ scaling for a fully-coherent search. (For an exact prediction, the details of StackSlide sensitivity [12] as well as both the overall and per-segment duty factors need to be accounted for.)

When going from the purely-Gaussian to the transient-line data set, the performance of $\hat{\mathcal{F}}$ and $\hat{B}_{S/GL}$ decreases somewhat more strongly for these tCW signals than it did for persistent signals, with $\hat{B}_{S/GL}$ losing up to 10% in p_{det} at some h_0 values and increasing to $h_0^{90\%}/\sqrt{S} \approx 0.12$.

Considering the permanence veto, we confirm that it would effectively remove almost all of these tCW signals, and hence we indeed need an alternative detection statistic for this case.

The Bayes factor $\hat{B}_{S/GLtL}$, which adds to $\hat{B}_{S/GL}$ only the possibility of transient single-detector disturbances (such as that in the second data set), but not of the multi-detector-coherent transient signals we are now injecting,

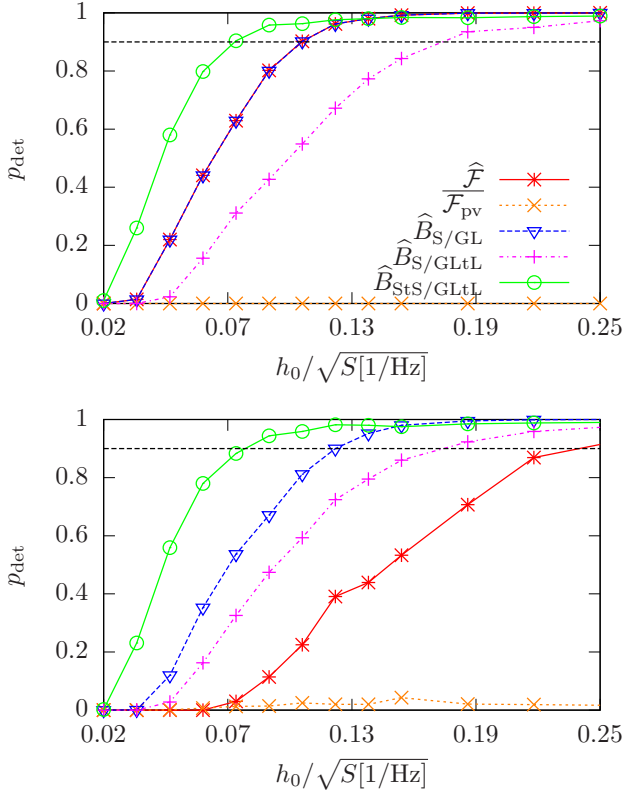


FIG. 5. Detection efficiency p_{det} for transient tCW signals with $T_{\text{inj}} = T_{\text{seg}} = 60\text{h}$, randomly distributed over segments, for the same statistics as in Fig. 4. The dashed horizontal lines marks $p_{\text{det}} = 90\%$. Top panel: injections in pure Gaussian noise, bottom panel: injections in Gaussian noise with a transient disturbance.

was found before to be safe for persistent CW signals. Now it turns out to be much safer for tCWs than the permanence veto, but still performs worse than $\widehat{B}_{S/GL}$ in both noise data sets, with $h_0^{90\%}/\sqrt{S} \approx 0.17$. Hence, this is not a particularly safe detection statistic for tCWs.

On the other hand, the full transient-signal-aware $\widehat{B}_{\text{StS/GLtL}}$ yields a significant increase in detection efficiency over $\widehat{B}_{S/GL}$, even in the second data set where a transient single-detector disturbance and transient signals are present together. It achieves $h_0^{90\%}/\sqrt{S} \approx 0.08$ in both data sets and yields up to 35% improvement in p_{det} for weak signals below this threshold.

Again, there are no losses with the simplified ‘loudest-only’ detection statistic $\widehat{B}_{\text{StS/GLtL},\text{lo}}$ only using the segment m with $\widetilde{\mathcal{F}}^m = \max_{\ell} \widetilde{\mathcal{F}}^{\ell}$ (not plotted separately).

However, a minor problem with $\widehat{B}_{\text{StS/GLtL}}$ is easy to overlook in Fig. 5. Even at very high h_0 , where other detection statistics eventually reach $p_{\text{det}} = 1$, it misses a few signal injections, typically about 1–2%.

We found that all missed injections are related to the previously-mentioned peculiarities of data selection, falling into segments 64 or 76, where one of the detectors

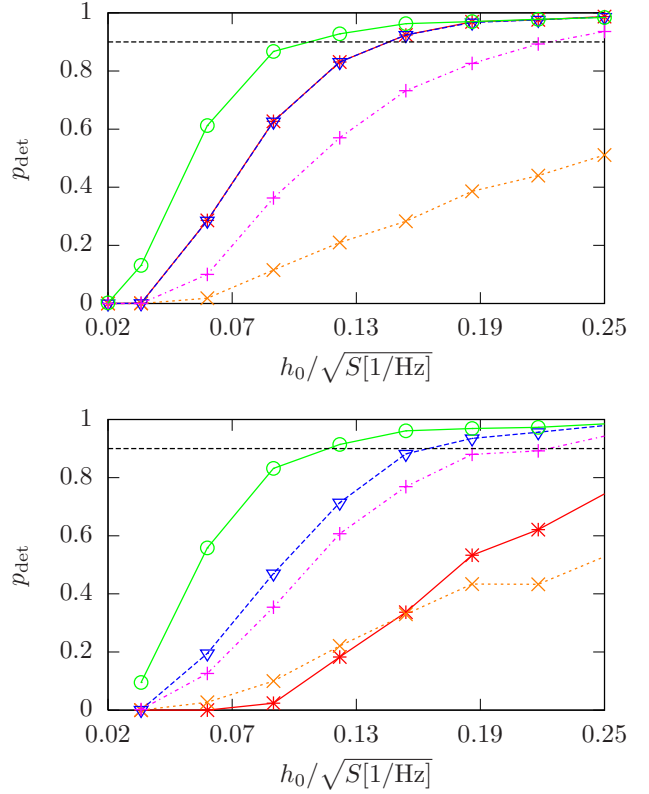


FIG. 6. Detection efficiency p_{det} for transient tCW signals of random duration $T_{\text{inj}} \in [0.5, 2.0] \times T_{\text{seg}}$ and randomly distributed over the whole observation time. Here, the signal amplitude h_0 has been *rescaled* for each injection to compensate for the varying T_{inj} , see text for details. Detection statistics and panels are the same as in Figs. 4 and 5.

contributes no or very little data.

Here, the single-segment hypotheses $\widetilde{\mathcal{H}}_{\text{tL}}^{X\ell}$ and $\widetilde{\mathcal{H}}_{\text{tS}}^{\ell}$ become indistinguishable, and the normalization of $\widehat{B}_{\text{StS/GLtL}}$ with the given tuning values is such that it will veto any strong outlier from these segments.

This issue is not a fundamental problem with our approach, as the data selection for future semicoherent searches can easily be constrained to avoid such anomalous segments, making the search better suited for tCW detection without risking optimality for persistent CWs.

As a simple work-around for the given data selection, we can simply set $\widetilde{o}_{\text{tL/G}}^{X\ell=64,76} = 0.0$ while keeping all other $\widetilde{o}_{\text{tL/G}}^{X\ell}$ at equal values. This makes $p_{\text{det}}(\widehat{B}_{\text{StS/GLtL}})$ go to 1 for high h_0 , just as $\widehat{B}_{S/GL}$ does, and sacrifices only 1–2% of p_{det} at lower h_0 , and a similar small amount in the persistent-CW case – which could also be recovered by slightly changing the $\mathcal{F}_*^{(0)}$ tuning.

D. tCW signals with varying duration

The pragmatic signal model for transient CW-like signals from Eq. (27) explicitly assumes a signal lining up

with a single segment, as tested in the previous section. As such an alignment is not very likely in nature, it is interesting to test the robustness of the new detection statistic against deviations from this assumption. Hence, we have also tested injecting transient signals with random lengths T_{inj} and with random start times uniformly drawn from $[t_{\text{start}}, t_{\text{end}} - T_{\text{inj}}]$.

For better comparison with Fig. 5, the strength of these signals is scaled according to $h_0 \propto \sqrt{T_{\text{seg}}/T_{\text{inj}}}$, so that the *average* signal-to-noise ratios for each nominal h_0 value are the same. (But note that the per-injection SNRs are not fixed, as they still depend on the three randomized amplitude parameters.)

As an example, we show the results for the Gaussian-noise data set, and for T_{inj} uniformly drawn from the interval $[0.5, 2.0] \times T_{\text{seg}} = [30, 120]\text{h}$, in Fig. 6. Here we find a general decrease in detection efficiency for all statistics considered, with $\hat{\mathcal{F}}$ and $\hat{B}_{\text{S/GL}}$ only achieving $h_0^{90\%}/\sqrt{S} \approx 0.14$ instead of ≈ 0.1 in the previous test and $\hat{B}_{\text{StS/GLtL}}$ achieving $h_0^{90\%}/\sqrt{S} \approx 0.1$ instead of ≈ 0.08 . This is mostly due to the fact that now a significant fraction of injections fall completely or partially within gaps of the simulated data set, or within parts with very low duty factor, thus decreasing the effective SNR for any detection method.

The main finding here is that the transient-aware Bayes factor $\hat{B}_{\text{StS/GLtL}}$ still improves over the other statistics, and that this is still true even for the approximate ‘loudest-only’ version. This indicates that, though the initial assumption of a tCW signal that exactly matches the duration of a single segment seemed quite strict and arbitrary, this simple approach is in fact useful for a wider range of tCW durations.

We also observe that the permanence veto is not quite as strict in falsely vetoing these tCW signals as it was for $T_{\text{inj}} = T_{\text{seg}}$, as some fraction of them that overlaps with more than one segment can now still contribute to the re-averaged detection statistic. Still, it is not competitive with any of the other tested detection statistics, which is no surprise, since it was not constructed to accept transient signals in the first place.

VI. CONCLUSIONS

In this paper, we have considered \mathcal{F} -statistic-based semicoherent CW searches on data that contains transient CW-like (quasi-monochromatic) signals or transient instrumental disturbances. We have generalized the Bayesian model-selection approach of Refs. [27, 36, 39] with explicit models for transients lasting for a single segment of a semicoherent search, including single-detector disturbances and multi-detector-coherent signals.

With injection studies on simulated data, using realistic duty factors corresponding to the two LIGO detectors during their sixth science run, we have shown that the new detection statistic $\hat{B}_{\text{StS/GLtL}}$ is *more robust* than standard semicoherent statistics towards both persistent

and transient single-detector disturbances in the data, while not hurting sensitivity to persistent CW signals, and that it is *more sensitive* towards transient signals.

We found that $\hat{B}_{\text{StS/GLtL}}$ works best if the transient signals or disturbances indeed last for exactly a single segment of the semicoherent search. But it still yields significant improvement over standard methods for transient durations shorter or longer than one segment length.

Though the injection studies showed a minor issue with $\hat{B}_{\text{StS/GLtL}}$ dismissing a small number of strong tCW signals, this was found to be related solely to a peculiarity of the data selection used in our tests. It can be worked around by prior tuning, while for future combined CW-tCW searches the issue can easily be avoided by a properly constrained data selection.

Just as with the line-robust statistic $B_{\text{S/GL}}$ of Ref. [36], the new detection statistic $\hat{B}_{\text{StS/GLtL}}$ only requires quantities that are already computed in any semicoherent \mathcal{F} -statistic search: namely the single-detector and single-segment \mathcal{F} -statistics. Hence, computational cost is only increased by the arithmetic operations in computing $\hat{B}_{\text{StS/GLtL}}$, as given in Eq. 23. Our injection studies showed that this is usually dominated by a few terms, and that good sensitivity can already be obtained by computing $\hat{B}_{\text{StS/GLtL}}$ only for the most significant candidates obtained from other statistics. Hence, these results allow for a CW search with increased robustness to transient disturbances and increased sensitivity to transient signals as a computationally cheap ‘add-on’ to existing searches, such as the Einstein@Home project [45].

The present approach could be further generalized to allow for an explicit classification of periodic data signatures into several classes (persistent CW signals, persistent lines, transient disturbances and ‘transient-CW’ signals), with transient lengths of any multiple of a segment length, through the *Bayesian Blocks* algorithm [48, 49].

Multi-detector transient disturbances cannot be safely distinguished from transient astrophysical signals by considering the per-segment and per-detector \mathcal{F} -statistics only. However, for widely-separated detectors these are much rarer than single-detector disturbances, and hence it should be possible to investigate any coincident transient candidates with more detailed analysis of their frequency evolution and coherence with auxiliary channels.

Sensitivity comparisons of tCW detection methods between this work, the dedicated tCW detection statistic of Ref. [27] and the ‘long-transient’ excess-power method of Ref. [35] might be an interesting goal for a mock-data challenge similar to the Sco-X1 comparison [50].

ACKNOWLEDGMENTS

I would like to thank Reinhard Prix for valuable advice throughout this project and for feedback on the manuscript; Berit Behnke, Maria Alessandra Papa, Ornella Piccinni, Irene Di Palma and Heinz-Bernd Eggenstein for analyses of LIGO S5 and S6 data that inspired

this study; the LIGO Scientific Collaboration for providing those data sets; Graham Woan, Ik Siong Heng and Eric Thrane for inspiring discussions about transient signals, Sinéad Walsh for advice on injection studies; and HB Eggenstein for plotting help. The injection studies on simulated data were carried out on the ATLAS cluster at AEI Hannover. This paper has been assigned document number LIGO-P1500159.

Appendix A: ‘cheat sheet’: pictorial representations of Bayes factors

In this appendix, we provide a simple pictorial representation of the various detection statistics (Bayes factors) derived from Bayesian hypothesis testing in Refs. [36, 39] and in this paper.

Here we consider the simplest example case that still allows distinguishing all of our hypotheses $\hat{\mathcal{H}}_G, \hat{\mathcal{H}}_S, \hat{\mathcal{H}}_L, \hat{\mathcal{H}}_{tS}$ and $\hat{\mathcal{H}}_{tL}$: this is the case of 2 detectors $X = 1, 2$ and 2 data segments $\ell = 1, 2$. We then represent with \square any hypothesis that posits pure Gaussian noise in the single-detector, single-segment data sub-set (X, ℓ) . Alternatively, \blacksquare depicts any hypothesis that posits a quasi-monochromatic signature, be it a signal or a disturbance, in (X, ℓ) .

- (i) a detection statistic that takes into account ‘transient lines’ in any single-detector, single-segment subset as an additional noise component in the denominator, given in Eq. (22), and which we can sketch as

$$\hat{B}_{S/GLtL}(\mathbf{x}) \propto \frac{P(\blacksquare\blacksquare|\mathbf{x})}{P(\square\square|\mathbf{x}) + P(\blacksquare\square|\mathbf{x}) + P(\square\blacksquare|\mathbf{x}) + P(\blacksquare\square|\mathbf{x}) + P(\square\blacksquare|\mathbf{x}) + P(\blacksquare\square|\mathbf{x}) + P(\square\blacksquare|\mathbf{x})}. \quad (\text{A4})$$

- (ii) another detection statistic, given in Eq. (34), that also takes into account ‘transient-CW’ signals in the numerator, which as a sketch looks like this:

$$\hat{B}_{StS/GLtL}(\mathbf{x}) \propto \frac{P(\blacksquare\blacksquare|\mathbf{x}) + P(\blacksquare\square|\mathbf{x}) + P(\square\blacksquare|\mathbf{x})}{P(\square\square|\mathbf{x}) + P(\blacksquare\square|\mathbf{x}) + P(\square\blacksquare|\mathbf{x}) + P(\blacksquare\square|\mathbf{x}) + P(\square\blacksquare|\mathbf{x}) + P(\blacksquare\square|\mathbf{x}) + P(\square\blacksquare|\mathbf{x})}. \quad (\text{A5})$$

We then build up sketches of the full semi-coherent hypothesis by arranging the 2 detectors on the horizontal axis and the 2 segments on the vertical axis.

This way, the signal-vs-Gaussian Bayes factor from Eq. (6), which is equivalent to the $\hat{\mathcal{F}}$ -statistic [39], can be represented (up to proportionality, corresponding to global priors) as

$$B_{S/G}(\mathbf{x}) \propto e^{\hat{\mathcal{F}}(\mathbf{x})} \propto \frac{P(\hat{\mathcal{H}}_S|\mathbf{x}, \mathcal{I})}{P(\hat{\mathcal{H}}_G|\mathbf{x}, \mathcal{I})} \propto \frac{P(\blacksquare\blacksquare|\mathbf{x})}{P(\square\square|\mathbf{x})}. \quad (\text{A1})$$

Using the same sketch notation, the pure line-veto statistic from Ref. [36], reads as

$$B_{S/L}(\mathbf{x}) \propto \frac{P(\blacksquare\blacksquare|\mathbf{x})}{P(\blacksquare\square|\mathbf{x}) + P(\square\blacksquare|\mathbf{x})}, \quad (\text{A2})$$

and the more general line-robust statistic, reproduced here in Eq. (13), is

$$B_{S/GL}(\mathbf{x}) \propto \frac{P(\blacksquare\blacksquare|\mathbf{x})}{P(\square\square|\mathbf{x}) + P(\blacksquare\square|\mathbf{x}) + P(\square\blacksquare|\mathbf{x})}. \quad (\text{A3})$$

In this paper, we have generalized the approach of Ref. [36] to yield

-
- [1] Abbott B P *et al.* (LIGO Scientific Collaboration) 2009 *Rep. Prog. Phys.* **72** 076901 [0711.3041]
[2] Grote H (for the LIGO Scientific Collaboration) 2010 *Class. Quant. Grav.* **27** 084003
[3] Accadia T *et al.* 2011 *Class. Quant. Grav.* **28** 114002
[4] Aasi J *et al.* 2015 *Class. Quant. Grav.* **32** 074001 [1411.4547]
[5] Acernese F *et al.* 2015 *Class. Quant. Grav.* **32** 024001 [1408.3978]
[6] Prix R (for the LSC) 2009 Gravitational waves from spinning neutron stars *Neutron Stars and Pulsars (Astrophysics and Space Science Library vol 357)* ed Becker W (Springer Berlin Heidelberg) p 651 ISBN 978-3-540-76964-4 (LIGO-P060039-v3) URL <https://dcc.ligo.org/LIGO-P060039/public>
[7] Johnson-McDaniel N K and Owen B J 2013 *Phys. Rev. D* **88** 044004 [1208.5227]
[8] Brady P R and Creighton T 2000 *Phys. Rev. D* **61** 082001 [gr-qc/9812014]
[9] Cutler C, Gholami I and Krishnan B 2005 *Phys. Rev. D* **72** 042004 [gr-qc/0505082]
[10] Krishnan B, Sintes A M, Papa M A, Schutz B F, Frasca S and Palomba C 2004 *Phys. Rev. D* **70** 082001 [gr-qc/0407001]
[11] Pletsch H J and Allen B 2009 *Phys. Rev. Lett.* **103** 181102 [0906.0023]
[12] Prix R and Shaltev M 2012 *Phys. Rev. D* **85** 084010 [1201.4321]
[13] Christensen N (for the LVC) 2010 *Class. Quant. Grav.* **27** 194010
[14] Coughlin M (for the LVC) 2010 *J. Phys. Conf. Ser.* **243** 012010 [1109.0330]
[15] Aasi J *et al.* (LIGO Scientific Collaboration and Virgo Collaboration) 2012 *Class. Quant. Grav.* **29** 155002

- [1203.5613]
- [16] Accadia T *et al.* 2012 *J. Phys. Conf. Ser.* **363** 012037
- [17] Aasi J *et al.* (LIGO Scientific Collaboration and Virgo Collaboration) 2013 *Phys. Rev. D* **87** 042001 [1207.7176]
- [18] Aasi J *et al.* (LIGO Scientific Collaboration and Virgo Collaboration) 2015 *Class. Quant. Grav.* **32** 115012 [1410.7764]
- [19] Aasi J *et al.* (LIGO Scientific Collaboration and Virgo Collaboration) 2013 *Phys. Rev. D* **88** 102002 [1309.6221]
- [20] Behnke B, Papa M A and Prix R 2015 *Phys. Rev. D* **91** 064007 [1410.5997]
- [21] Behnke B 2013 *A Directed Search for Continuous Gravitational Waves from Unknown Isolated Neutron Stars at the Galactic Center* Ph.D. thesis Leibniz Universität Hannover URL <http://opac.tib.uni-hannover.de/DB=1/XMLPRS=N/PPN?PPN=752172840>
- [22] Pletsch H J 2008 *Phys. Rev. D* **78** 102005 [0807.1324]
- [23] Piccinni O 2014 *Mitigation of transient disturbances in wide parameter space searches for continuous gravitational wave signals* Master's thesis Università di Roma La Sapienza
- [24] Blackburn L *et al.* 2008 *Class. Quant. Grav.* **25** 184004 [0804.0800]
- [25] Slutsky J *et al.* 2010 *Class. Quant. Grav.* **27** 165023 [1004.0998]
- [26] Prestegard T, Thrane E, Christensen N L, Coughlin M W, Hubbert B, Kandhasamy S, MacAyeal E and Mandic V 2012 *Class. Quant. Grav.* **29** 095018 [1111.1631]
- [27] Prix R, Giampanis S and Messenger C 2011 *Phys. Rev. D* **84** 023007 [1104.1704]
- [28] Santiago Prieto R I 2014 *Transient Gravitational Waves at r-mode Frequencies from Neutron Stars* Ph.D. thesis University of Glasgow
- [29] Lyne A G, Shemar S L and Smith F G 2000 *Mon. Not. R. Astron. Soc.* **315** 534–542
- [30] van Eysden C A and Melatos A 2008 *Class. Quant. Grav.* **25** 225020 [0809.4352]
- [31] Bennett M F, van Eysden C A and Melatos A 2010 *Mon. Not. R. Astron. Soc.* **409** 1705–1718 [1008.0236]
- [32] Levin Y and van Hoven M 2011 *Mon. Not. R. Astron. Soc.* **418** 659–663 [1103.0880]
- [33] Kashiyama K and Ioka K 2011 *Phys. Rev. D* **83** 081302 [1102.4830]
- [34] Singh A *Gravitational Wave transient signal emission (CW-transients) during post-glitch relaxation phase of a Neutron Star* in preparation
- [35] Thrane E, Mandic V and Christensen N 2015 *Phys. Rev. D* **91** 104021 [1501.06648]
- [36] Keitel D, Prix R, Papa M A, Leaci P and Siddiqi M 2014 *Phys. Rev. D* **89** 064023 [1311.5738]
- [37] Jaranowski P, Królak A and Schutz B F 1998 *Phys. Rev. D* **58** 063001 [gr-qc/9804014]
- [38] Cutler C and Schutz B F 2005 *Phys. Rev. D* **72** 063006 [gr-qc/0504011]
- [39] Prix R and Krishnan B 2009 *Class. Quant. Grav.* **26** 204013 [0907.2569]
- [40] Abbott B *et al.* (LIGO Scientific Collaboration) 2004 *Phys. Rev. D* **69** 082004 [gr-qc/0308050]
- [41] Prix R 2007 *Phys. Rev. D* **75** 023004 [gr-qc/0606088]
- [42] Jaynes E T 2003 *Probability Theory. The Logic of Science* (Cambridge University Press)
- [43] Keitel D and Prix R 2015 *Class. Quant. Grav.* **32** 035004 [1409.2696]
- [44] Shaltev M 2013 *Optimization and follow-up of semi-coherent searches for continuous gravitational waves* Ph.D. thesis Leibniz Universität Hannover URL <http://opac.tib.uni-hannover.de/DB=1/XMLPRS=N/PPN?PPN=755483928>
- [45] Allen B *et al.* Einstein@Home distributed computing project URL <http://einsteinathome.org/>
- [46] Aasi J *et al.* (LIGO Scientific Collaboration and Virgo Collaboration) *Einstein@Home search for continuous gravitational waves in LIGO S6 data* in preparation
- [47] LSC Algorithm Library - LALSuite (free software) URL <https://www.lsc-group.phys.uwm.edu/daswg/projects/lalsuite.html>
- [48] Scargle J D 1998 *Astrophys. J.* **504** 405–418 [astro-ph/9711233]
- [49] Scargle J D, Norris J P, Jackson B and Chiang J 2013 *Astrophys. J.* **764** 167 [1207.5578]
- [50] Messenger C *et al.* 2015 *Phys. Rev. D* **92** 023006 [1504.05889]